

文章编号: 1001 - 9014(2008)02 - 0081 - 05

QUANTUM EFFICIENCY OPTIMIZATION OF InP-BASED $\text{In}_{0.53}\text{Ga}_{0.47}\text{As}$ PHOTODETECTORS

TIAN Zhao-Bing^{1,2}, GU Yi^{1,2}, ZHANG Yong-Gang¹

- (1. State Key Laboratory of Functional Materials for Informatics, Shanghai Institute of Microsystem and Information Technology, Chinese Academy of Sciences, Shanghai 200050, China;
2. Postgraduate School, Chinese Academy of Sciences, Beijing 100039, China)

Abstract: A modified physical model on the optical response of InP-based $\text{In}_{0.53}\text{Ga}_{0.47}\text{As}$ PN photodetectors was presented. By introducing a collecting factor, the optical response and quantum efficiency were simulated. The influences of device parameters on quantum efficiency of typical $\text{In}_{0.53}\text{Ga}_{0.47}\text{As}/\text{InP}$ PN photodetectors under both front and backside illuminated conditions were investigated by using our model. Furthermore, two modified InGaAs/InP PD structures for back-illumination were proposed, and the optimal structural parameters were discussed.

Key words: short-wave-infrared; photovoltaic detectors; InGaAs; quantum efficiency

CLC number: TN2 **Document:** A

InP基 $\text{In}_{0.53}\text{Ga}_{0.47}\text{As}$ 光电探测器的量子效率优化

田招兵^{1,2}, 顾溢^{1,2}, 张永刚¹

- (1. 中国科学院上海微系统与信息技术研究所 信息功能材料国家重点实验室, 上海 200050;
2. 中国科学院研究生院, 北京 100039)

摘要: 建立了不同结构的 InP 基 PN 型 $\text{In}_{0.53}\text{Ga}_{0.47}\text{As}$ 探测器光响应的物理模型. 通过引入收集效率函数, 模拟计算了探测器量子效率和光响应. 采用该模型分别研究了正面进光和背面进光情况下典型的 $\text{In}_{0.53}\text{Ga}_{0.47}\text{As}/\text{InP}$ PN 探测器的结构参数对器件量子效率的影响. 在此基础上提出了两种改进的背照射 InGaAs/InP 探测器结构, 并讨论了其结构参数的优化.

关键词: 短波红外; 光伏型探测器; InGaAs; 量子效率

Introduction

InP-based short-wave-infrared (SWIR) InGaAs photodetectors (PDs) and their arrays^[1-3] have been used in various applications including remote sensing and imaging^[11], where high sensitivity and low-noise are two key points of concern. The quantum efficiency (QE) and the responsivity, as well as the dark current, are the most important device parameters of the PDs. The dark current behavior of InGaAs PDs has been extensively studied in our previous works^[4-6].

In this paper, a modified physical model used for QE optimization of InP-based $\text{In}_{0.53}\text{Ga}_{0.47}\text{As}$ PDs is demonstrated. In this model, a collecting factor is introduced and proper parameters of the materials are adopted. Based on this model, the QE of typical $\text{In}_{0.53}\text{Ga}_{0.47}\text{As}/\text{InP}$ PN PDs under front and backside illuminated conditions with different doping levels and the thicknesses of absorbing layer are investigated in detail. Furthermore, two modified structures for back-illumination are proposed, and the relationships of their structural parameters with QE are simulated.

Received date: 2007 - 11 - 15, **revised date:** 2007 - 12 - 26

收稿日期: 2007 - 11 - 15, **修回日期:** 2007 - 12 - 26

Foundation item: Knowledge innovation program of Chinese Academy of Sciences, Shanghai STC Project (06ZR14104) and SMTEC Project

Biography: TIAN Zhao-Bing, (1981-), male, Xi'an, Shaanxi, China. Candidate for doctor degree, research area is semiconductor optoelectronic devices.

1 Physical model and parameters

In PN PDs, photo-carriers induced by incident photons ($h > Eg$) are separated by the electric field to the opposite side of the junction, and consequently photo-current is generated. The photo-current consists of two parts: photo-carriers generated in the depletion layer, and photo-carriers generated outside the depletion region that diffused into the depletion layer^[7].

For typical $In_{0.53}Ga_{0.47}As/InP$ PDs as schematically shown in Fig 1, the generation rate $g_1(x)$ of electron-hole pairs in $In_{0.53}Ga_{0.47}As$ absorbing layer is given by^[7]

$$g_1(x) = P(x) \cdot \alpha_1 = P_0 \cdot e^{-\alpha_2 d_2} \cdot e^{-\alpha_1 x} \cdot \alpha_1 \quad (1)$$

where P_0 is the incident light power, α_1 and α_2 are the absorption coefficient of $In_{0.53}Ga_{0.47}As$ and InP , respectively.

Since electrons and holes in the depletion layer are moving very fast in the electric field, recombination in the depletion region is negligible^[8]. And the influence of band discontinuity on carrier transport at the junction is also neglected in our model^[7]. Therefore the collecting factor $\eta(x)$ in the depletion region is close to unity. Assuming the collecting factor outside the depletion layer decreases exponentially with the minority carrier diffusion length L_{h1} , $\eta_1(x)$ in the $In_{0.53}Ga_{0.47}As$ layer can be written as

$$\eta_1(x) = \begin{cases} 1, & 0 \leq x \leq d_1 \\ e^{-x/L_{h1}}, & d_1 < x \leq d_1 + l_1 \end{cases} \quad (2)$$

The photocurrent contributed from the $n^- - In_{0.53}Ga_{0.47}As$ absorber layer is

$In_{0.53}Ga_{0.47}As$ absorber layer is

$$J_{R1} = \int_0^{d_1} g(x) \cdot \eta_1(x) dx \quad (3)$$

Similarly, the photo-current contributed from $P^+ - InP$ cap layer can be deduced. Thus the total photo-current could be calculated.

Careful choice of the material parameters is of great importance in acquiring accurate modeling predictions^[7,8], especially the key electrical and optical parameters, such as minority-carrier lifetime, mobility, absorption coefficient, etc. Some widely investigated III-V material parameters are available in related papers^[9-12] and handbooks^[13,14], yet others still lack of reliable data. Among these key parameters, the minority carrier lifetime (τ) and absorption coefficient (α) have direct effects on modeling accuracy.

The minority-carrier lifetime of $In_{0.53}Ga_{0.47}As$ as a function of carrier concentration used in our simulation is plotted in Fig 2, where the quasi-empirical model proposed by R. K. Ahrenkie^[15] is adopted in combination with the consideration of photon recycling effect^[16] of double heterostructures by introducing a recycling factor of 10^[17,18]. The values of some key parameters used in our simulation are summarized in Table 1.

2 QE optimization

$InGaAs$ PDs for optical communication applications emphasize particularly on the frequency characteristic, then the QE and dark current. While for remote sensing applications, the QE and dark-current are the primary concern. In array applications the total noise

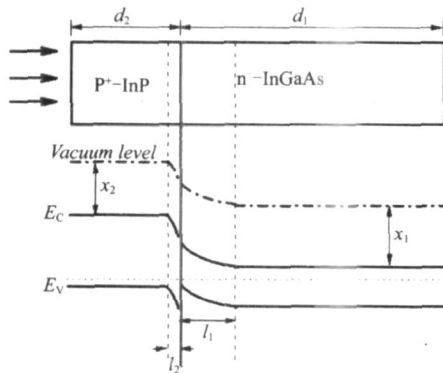


Fig 1 Schematics of front illuminated $In_{0.53}Ga_{0.47}As$ PN photodetector

图 1 正入射 $In_{0.53}Ga_{0.47}As$ PN探测器示意图

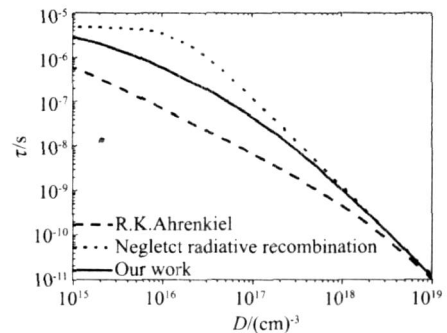


Fig 2 $In_{0.53}Ga_{0.47}As$ minority-carrier lifetime as a function of doping concentration D at 300K

图 2 300K下 $In_{0.53}Ga_{0.47}As$ 少子寿命与掺杂浓度 D 的关系

表 1 Some key parameters of $\text{In}_{0.53}\text{Ga}_{0.47}\text{As}$ and InP used in our calculations

Table 1 计算中用到的 $\text{In}_{0.53}\text{Ga}_{0.47}\text{As}$ 和 InP材料的部分关键参数

	P ⁺	InP $\text{In}_{0.53}\text{Ga}_{0.47}\text{As}$
@ 1.65 μm (cm^{-1})	5 ^[10, 11, 14]	2.9 $\times 10^4$ ^[13]
E_g (eV)	1.331 ^A	0.74
N_c (cm^{-3})	5.72 $\times 10^{17}$	2.08 $\times 10^{17}$
N_v (cm^{-3})	1.14 $\times 10^{19}$	7.56 $\times 10^{18}$
D_e (cm^2/s)	130	300
D_h (cm^2/s)	5	7.5
(ns)	0.5 ^{[12]B}	See Fig 2

A: band-gap narrowing due to heavily doping is considered

B: of n-doped InP is $1 \sim 2\text{ns}^{[13]}$, 1ns is adopted in our simulation

arises from both the PDs and the read-out circuit (ROC). In lattice matched case, the total noise is usually dominated by ROC rather than PDs, therefore the optimization of QE becomes the main concern.

Since the optical response of PDs mainly comes from InGaAs absorbing layer, which is directly proportional to QE, the influence of i-layer parameters (i.e. i-layer thickness and doping concentration) on the internal QE of these $\text{In}_{0.53}\text{Ga}_{0.47}\text{As}$ PDs around peak wavelength is mainly investigated in this paper.

2.1 Front-illuminated InGaAs PD

The influence of i-layer thickness and doping concentration on internal QE of front illuminated $\text{In}_{0.53}\text{Ga}_{0.47}\text{As}$ PDs is shown in Fig 3. The QE decreases slowly as the doping concentration increases, and increases monotonously with i-layer thickness until saturation occurs. It could be deduced that, under front illuminated condition, i-layer thickness of 1.5 ~ 2 (μm) is thick enough to reach higher QE, whereas the optimal doping concentration should be a trade-off between QE and dark current. When the PD with n⁻- $\text{In}_{0.53}\text{Ga}_{0.47}\text{As}$ thicker than 1.5 μm and doping concentration around $2 \sim 5\text{E}16\text{cm}^{-3}$, internal QE above 90% could be achieved.

2.2 Back-illuminated InGaAs PD

As shown in Fig 4, as for typical $\text{In}_{0.53}\text{Ga}_{0.47}\text{As}/\text{InP}$ PD under back-illumination, the internal QE firstly increases with the augment of i-InGaAs layer thickness d_i and then decreases as d_i gets thicker. The higher the i-layer doping concentration is, the faster the QE decreases as i-layer becomes thicker. Simulation results indicate that the internal QE around 80% could

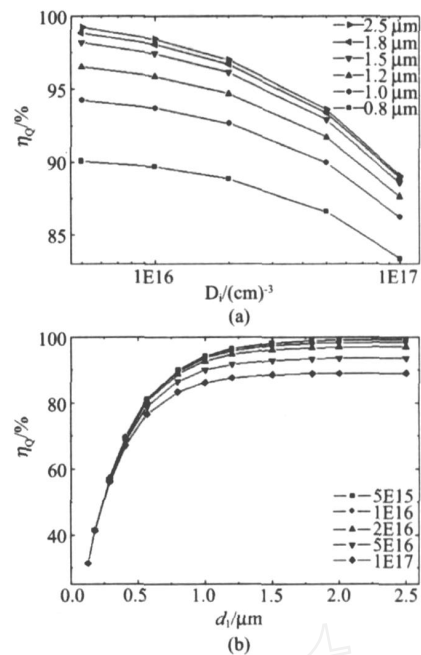


Fig 3 Internal quantum efficiency η_Q of front-illuminated typical PN InGaAs/InP PD as a function of (a) i-layer doping concentration D_i at various i-layer thicknesses (b) i-layer thickness d_i with different i-layer doping concentrations. 图 3 正进光时 PN型 InGaAs/InP 探测器内量子效率 η_Q (a)在不同 i 层厚度下与 i 层掺杂浓度 D 的关系 (b)在不同 i 层掺杂下与 i 层厚度 d 的关系

be achieved when the back-illuminated $\text{In}_{0.53}\text{Ga}_{0.47}\text{As}$ PD with n⁻-InGaAs thickness around 0.8 ~ 1.2 μm and doping concentration below $5\text{E}16\text{cm}^{-3}$.

2.3 Two other structures for back illumination

It is noticed from above analysis that for typical $\text{In}_{0.53}\text{Ga}_{0.47}\text{As}/\text{InP}$ PDs under backside illumination, optimal QE requires a relatively thin n⁻-InGaAs absorbing layer. But a thinner absorbing layer is not sufficient for collecting all incident photons. Hence, it is not suitable for the required high-sensitivity applications.

In order to further improve the internal QE of $\text{In}_{0.53}\text{Ga}_{0.47}\text{As}$ PDs for back illumination, homojunction or multi-layer heterostructures can be used. However, PDs with homojunctions suffer from soft reverse IV characteristics which results in a higher dark current. Here a modified structure with a thin InP barrier layer inserting between the p-InGaAs and n-InGaAs layers is adopted. The InP barrier would slightly reduce the optical response from the upper-InGaAs layer (when the lower-InGaAs layer thickness $> 1\mu\text{m}$, the QE comes

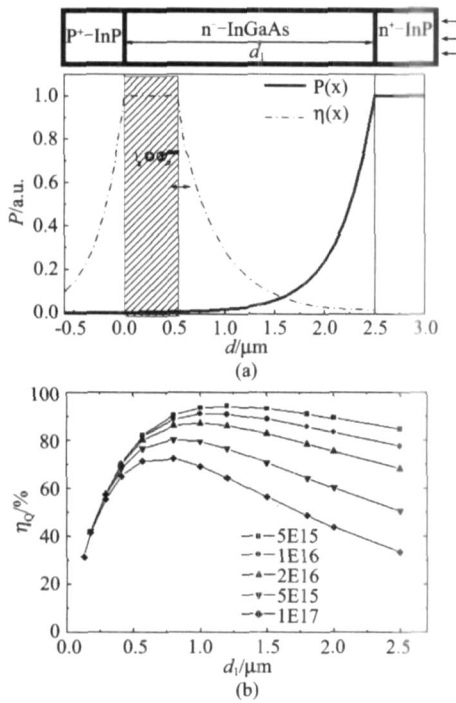


Fig 4 (a) Schematics of InGaAs/InP PD under back illumination, where P is the light power and d is the distance (b) internal quantum efficiency η_Q of InGaAs/InP PN PD as a function of i-InGaAs thickness d_i at various doping concentrations
图 4 (a) InGaAs/InP探测器背面照射示意图,其中 P 为光功率, d 为距离 (b) InGaAs/InP双异质结型PN探测器在背面照射时内量子效率 η_Q 在不同掺杂浓度情况下随 i 层厚度 d_i 的变化情况

from the upper-InGaAs (<2%), but it would effectively block the photo-carriers to diffuse towards the surface, thus the surface recombination would be greatly suppressed. The QE of two modified structures for back illumination based upon above analysis is calculated. The influence of structural parameters on internal QE is also investigated.

The structure 1 is a n-on-p stack as shown in Fig 5. The doping concentration of P⁺-InP cap layer is set as 2E18cm⁻³. The influence of n⁻-InGaAs absorbing layer thickness at various doping concentrations on QE is calculated. As plotted in Fig 5, the total QE increases logarithmically with n⁻-InGaAs thickness, and the contribution of N⁺-InGaAs cap layer becomes negligible when the absorbing layer is thicker than about 1μm. Considering the trade-off between the QE and dark current, an internal QE above 95% can be achieved in the back-illuminated PD1 with n⁻-In_{0.53}Ga_{0.47}As layer thicker than 1.5μm and doping concen-

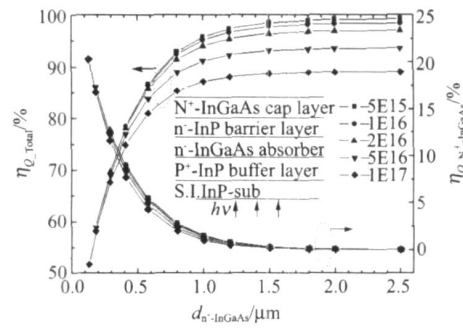


Fig 5 The influence of i-layer thickness $d_{n\text{-InGaAs}}$ and doping concentration on internal quantum efficiency η_{Q_Total} and $\eta_{Q_N^+-InGaAs}$ of back-illuminated InGaAs/InP PD1, the insert is schematic drawing of back-illuminated PD structure 1
图 5 背照射 PD1内量子效率 η_{Q_Total} 和 $\eta_{Q_N^+-InGaAs}$ 与 i 层厚度 $d_{n\text{-InGaAs}}$ 和掺杂浓度的关系,插图为背照射结构 PD1的示意图

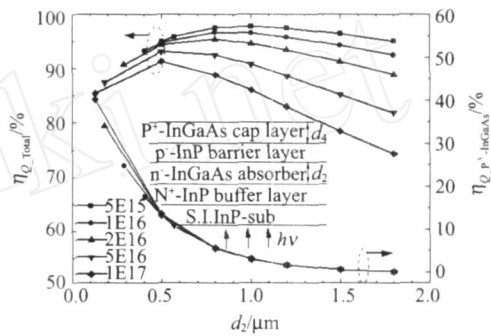


Fig 6 The influence of structural parameters on internal quantum efficiency η_{Q_Total} and $\eta_{Q_P^+-InGaAs}$ of back-illuminated InGaAs/InP PD2, the insert shows schematic drawing of back-illuminated PD structure 2
图 6 背入射结构 PD2中 n⁻-InGaAs层结构参数对内量子效率 η_{Q_Total} 与 $\eta_{Q_P^+-InGaAs}$ 的影响,插图为背入射结构 PD2示意图

tration around 2~5E16cm⁻³.

The structure 2 with a p-on-n configuration for back-illumination is schematically shown in Fig 6. The 0.2μm p-InP barrier layer doped to 1E18cm⁻³ is kept constant in our simulation. And the total thickness of n⁻-InGaAs and P⁺-InGaAs layer is assumed to be 2μm.

As shown in Fig 6, with the increase of d_2 , the total QE firstly increase and then decreases slowly. The contribution from P⁺-InGaAs layer decreases with the increase of n⁻-InGaAs layer thickness. The internal QE of 90% could be achieved with the thickness of n⁻-InGaAs layer around 0.5~1.0μm and the doping concentration around 2E16cm⁻³, and moderate dark

current characteristic could also be expected. The p-InP barrier layer concentration also has a slight influence on internal QE, which is found to be appropriate at higher doping levels. However, considering the inter-diffusion effect during the growth, the concentration of p-InP barrier layer around $5\text{E}17 \sim 1\text{E}18\text{cm}^{-3}$ is preferable.

3 Conclusions

In conclusion, a physical model of PN PDs for optical response optimization is established. The optical response properties of several lattice-matched InGaAs/InP PD structures under front and backside illuminated configurations are investigated in detail, and the optimal parameters for higher QE are also discussed. Combining this model with dark current analysis^[4-6], further optimization on SNR and detectivity of InGaAs/InP PN PDs and arrays could be realized.

REFERENCES

- [1] Martin T, Brubaker R, Dixon P, *et al.* 640 × 512 InGaAs focal plane array camera for visible and SW IR imaging [J]. *Proceedings of SPIE*, 2005, **5783**: 12—20.
- [2] LV Yan-Qiu, XU Yun-Hua, HAN Bing, *et al.* Study on 128 element linear InGaAs short wavelength infrared focal plane array [J]. *J. Infrared Millim. Waves* (吕行秋, 徐运华, 韩冰, 等. 128 × 1 线列 InGaAs 短波红外焦平面的研究. *红外与毫米波学报*), 2006, **25** (5): 333—337.
- [3] ZHANG Yong-Gang, GU Yi, ZHU Cheng, *et al.* Fabrication of short wavelength infrared InGaAs/InP photovoltaic detector series [J]. *J. Infrared Millim. Waves* (张永刚, 顾溢, 朱诚, 等. 短波红外 InGaAs/InP 光伏探测器系列的研究. *红外与毫米波学报*), 2006, **25** (1): 6—9.
- [4] HAO Guo-Qiang, ZHANG Yong-Gang, LU Tian-Dong, *et al.* The dark current characteristics of InGaAs PN photodetectors [J]. *Chin. J. Semiconductor Optoelectronics* (郝国强, 张永刚, 刘天东, 等. InGaAs PN 光电探测器的暗电流特性研究. *半导体光电*), 2004, **25** (5): 341—344.
- [5] HAO Guo-Qiang, ZHANG Yong-Gang, GU Yi, *et al.* Temperature behavior of InGaAs PN photodetectors [J]. *Chin. J. Functional Materials and Devices* (郝国强, 张永刚, 顾溢, 等. In_{0.53}Ga_{0.47}As PN 光电探测器的温度特性分析. *功能材料与器件学报*), 2005, **11** (2): 192—196.
- [6] HAO Guo-Qiang, ZHANG Yong-Gang, GU Yi, *et al.* Performance analysis of extended wavelength InGaAs photovoltaic detectors grown with gas source MBE [J]. *J. Infrared Millim. Waves* (郝国强, 张永刚, 顾溢, 等. 气态源分子束外延波长扩展 InGaAs 探测器性能分析. *红外与毫米波学报*), 2006, **25** (4): 241—245.
- [7] Emziane M, Nicholas R J. Optimization of InGaAs(P) photovoltaic cells lattice matched to InP [J]. *J. Appl. Phys.*, 2007, **101**: 054503.
- [8] Lal R, Jain M, Gupta S, *et al.* An analytical model of a double hetero-structure mid-infrared photodetector [J]. *Infrared Phys. Tech.*, 2003, **44**: 125—132.
- [9] Burkhard H, Dinges H, Kuphal E. Optical properties of InGaPAs, InP, GaAs, and GaP determined by ellipsometry [J]. *J. Appl. Phys.*, 1982, **53** (1): 655—662.
- [10] Zielinski E, Schweizer H, Streubel K, *et al.* Excitonic transitions and exciton damping processes in InGaAs/InP [J]. *J. Appl. Phys.*, 1986, **59** (6): 2196—2204.
- [11] Sobodeh M, Khalid A, Rezazadeh A. Empirical low-field mobility model for III-V compounds applicable in device simulation codes [J]. *J. Appl. Phys.*, 2000, **87** (6): 2890—2900.
- [12] Rosenwaks Y, Tsimberova I, Gerö H, *et al.* Minority-carrier recombination in p-InP single crystals [J]. *Phys. Rev. B*, 2003, **68**: 115210.
- [13] Levinshstein M, Rumyantsev S, Shur M. Handbook Series on Semiconductor Parameters [M] Vol 1. & Vol 2, Singapore: World Scientific, 1999.
- [14] Adachi S. *Physical Properties of III-V Semiconductor Compounds* [M]. New York: Wiley, 1992.
- [15] Ahrenkiel R, Ellingson R, Johnston S, *et al.* Recombination lifetime of InGaAs as a function of doping density [J]. *Appl. Phys. Lett.*, 1998, **72** (26): 3470—3472.
- [16] Dumke W. Spontaneous radiative recombination in semiconductors [J]. *Phys. Rev.*, 1957, **105**: 139—144.
- [17] Monte A, Silva S, Cruz J, *et al.* Spatial and temperature dependence of carrier recombination in an InGaAs/InP heterostructure [J]. *J. Appl. Phys.*, **85** (5): 2866—2869, 1999.
- [18] Ahrenkiel R, Keyes B, Durbin S, *et al.* Recombination lifetime and performance of III-V compound photovoltaic devices [C]. 23rd IEEE Photovoltaic Specialists Conference, Louisville, KY, USA, 1993, 42—51.